Protein Science (1999), *8*:1423–1431. Cambridge University Press. Printed in the USA.

Antibody variable region binding by *Staphylococcal* protein A: Thermodynamic analysis and location of the Fv binding site on E-domain

MELISSA A. STAROVASNIK, MARK P. O'CONNELL, WAYNE J. FAIRBROTHER, AND ROBERT F. KELLEY

Department of Protein Engineering, Genentech, Inc., One DNA Way, South San Francisco, California 94080

(RECEIVED January 12, 1999; ACCEPTED March 3, 1999)

Abstract

Immunoglobulins of human heavy chain subgroup III have a binding site for *Staphylococcal* protein A on the heavy chain variable domain (V_H), in addition to the well-known binding site on the Fc portion of the antibody. Thermodynamic characterization of this binding event and localization of the Fv-binding site on a domain of protein A is described. Isothermal titration calorimetry (ITC) was used to characterize the interaction between protein A or fragments of protein A and variants of the hu4D5 antibody Fab fragment. Analysis of binding isotherms obtained for titration of hu4D5 Fab with intact protein A suggests that 3–4 of the five immunoglobulin binding domains of full length protein A can bind simultaneously to Fab with a K_a of $5.5 \pm 0.5 \times 10^5$ M^{-1}. A synthetic single immunoglobulin binding domain, Z-domain, does not bind appreciably to hu4D5 Fab, but both the E and D domains are functional for hu4D5 Fab binding. Thermodynamic parameters for titration of the E-domain with hu4D5 Fab are $n = 1.0 \pm 0.1$, $K_a = 2.0 \pm 0.3 \times 10^5$ M^{-1}, and $\Delta H = -7.1 \pm 0.4$ kcal mol^{-1}. Similar binding thermodynamics are obtained for titration of the isolated V_H domain with E-domain indicating that the E-domain binding site on Fab resides within V_H. E-domain binding to an IgG1 Fc yields a higher affinity interaction with thermodynamic parameters $n = 2.2 \pm 0.1$, $K_a > 1.0 \times 10^7$ M^{-1}, and $\Delta H = -24.6 \pm 0.6$ kcal mol^{-1}. Fc does not compete with Fab for binding to E-domain indicating that the two antibody fragments bind to different sites. Amide ^1H and ^{15}N resonances that undergo large changes in NMR chemical shift upon Fv binding map to a surface defined by helix-2 and helix-3 of E-domain, distinct from the Fc-binding site observed in the crystal structure of the B-domain/Fc complex. The Fv-binding region contains negatively charged residues and a small hydrophobic patch which complements the basic surface of the region of the V_H domain implicated previously in protein A binding.

Keywords: calorimetry; IgG binding domains; NMR chemical shift mapping; *Staphylococcal* protein A

Staphylococcal protein A is a component of the cell surface of *Staphylococcus aureus*. The biological role of protein A is not understood fully, although it is secreted by nearly all clinical isolates of *S. aureus* and is thought to enhance pathogenicity (for review see Langone, 1982; Silverman, 1998; and references therein). Protein A interacts with antibodies through two distinct binding events: the "classical" binding site on the Fc portion of human IgG1, IgG2, and IgG4, and the "alternate" binding site found on the Fab portion of human IgG, IgM, IgA, and IgE that contain heavy chains of the V_H3 subfamily. Protein A has long been studied for its properties as a valuable immunological tool and more recently for its ability to act as a B cell superantigen by cross-linking IgM molecules through V_H3-mediated binding (Romagnani et al., 1982).

Protein A is a 42 kDa protein containing five homologous ~58 residue immunoglobulin(Ig)-binding domains followed by a C-terminal region necessary for cell wall attachment. The Ig-binding domains are designated E, D, A, B, and C (in order from the N-terminus) and share 65–90% amino acid sequence identity. The domains were named based on the order in which they were discovered: A-, B-, and C-domains were initially identified as proteolytically stable modules (Hjelm et al., 1975; Sjödahl, 1976); D-domain was identified using modified digestion conditions (Sjödahl, 1977a, 1977b), and finally E-domain was recognized as an additional homologous Ig-binding domain when partial and complete cDNA clones were identified (Löfdahl et al., 1983; Uhlén et al., 1984; Moks et al., 1986).

NMR structures of isolated B-, E-, and Z-domains (a B-domain mutant; Nilsson et al., 1987) reveal that the individual modules are

Reprint requests to: Dr. Melissa A. Starovasnik, Department of Protein Engineering, Genetech, Inc., One DNA Way, South San Francisco, California 94080; e-mail: star@gene.com.

composed of three-helix bundle structures (Gouda et al., 1992; Tashiro & Montelione, 1995; Starovasnik et al., 1996; Tashiro et al., 1997). Residues from the first two helices are important for Fc binding (Cedergren et al., 1993; Jendeberg et al., 1995) and were shown to make contact with Fc in the B-domain/Fc crystal structure (Deisenhofer, 1981). Furthermore, a minimized protein A domain variant containing only the first two helices indicates that this region is not only necessary, but sufficient for high affinity Fc binding (Braisted & Wells, 1996; Starovasnik et al., 1997).

Less is known about the protein A/V_H3 interaction, however recently, all five protein A domains were shown to be capable of Fab binding with association constants of 2–14 $\times$ 10^6 M^{-1} (Roben et al., 1995; Jansson et al., 1998). Fab and Fc are noncompetitive for binding to the isolated D-domain (Roben et al., 1995), but the specific area on a protein A domain that interacts with V_H3 has not been determined. On the V_H3 side of the interaction, framework regions 1 and 3 and a portion of complementarity determining region 2 have been implicated as regions that interact with protein A based on swap mutations (Randen et al., 1993; Potter et al., 1996). Framework regions 1 and 3 of an isolated V_H3 domain were shown to be involved in protein A binding as monitored by NMR spectroscopy (Riechmann & Davies, 1995).

We report thermodynamic characterization of the interaction between protein A and the variable region of IgG. Complexes formed using full length protein A, a two domain E–D fragment, and the individual E-domain were investigated. Furthermore, the Fv binding site on the E-domain was localized by NMR chemical shift mapping.

Results

Thermal denaturation of protein A fragments

The stabilities of E-domain and the E–D two domain fragment of protein A were determined by differential scanning calorimetry (DSC). As shown in Figure 1A, E-domain is fairly unstable, exhibiting a melting temperature (T_m) of 43 °C at pH 5.0. Similar transitions were obtained upon consecutive heating cycles, indicating that denaturation is reversible, although the protein solution was turbid upon removal from the calorimeter cell. Melting of E-domain is not adequately described by a two-state model since $\Delta H_{cal}/\Delta H_{VH}$ is <1. A ΔH_{VH} that is larger than ΔH_{cal} is consistent with oligomerization upon unfolding (Privalov, 1979). A similar T_m was determined by thermal denaturation monitored by changes in ellipticity at 222 nm (data not shown). The low stability of E-domain limits the temperature range for binding measurements to ambient and below.

A single, broad transition having a T_m of 51.5 °C was observed for thermal denaturation of the E–D fragment as shown in Figure 1B. Like E-domain, denaturation of this fragment was found to be reversible. A similar broad transition was also detected by ellipticity measurements at 222 nm (data not shown). As for E-domain, the E–D fragment did not display two-state unfolding. Analysis of the transition with a non-two-state model yielded a ΔH_{VH} that was smaller than ΔH_{cal} suggesting the presence of folding intermediates. These results are consistent with a model whereby D-domain is slightly more stable than E-domain, and the two domains fold independently without strong interdomain interactions. Folding intermediates would thus consist of molecules having one domain folded and the other unfolded. No evidence was obtained for aggregation of the thermally denatured E–D fragment.

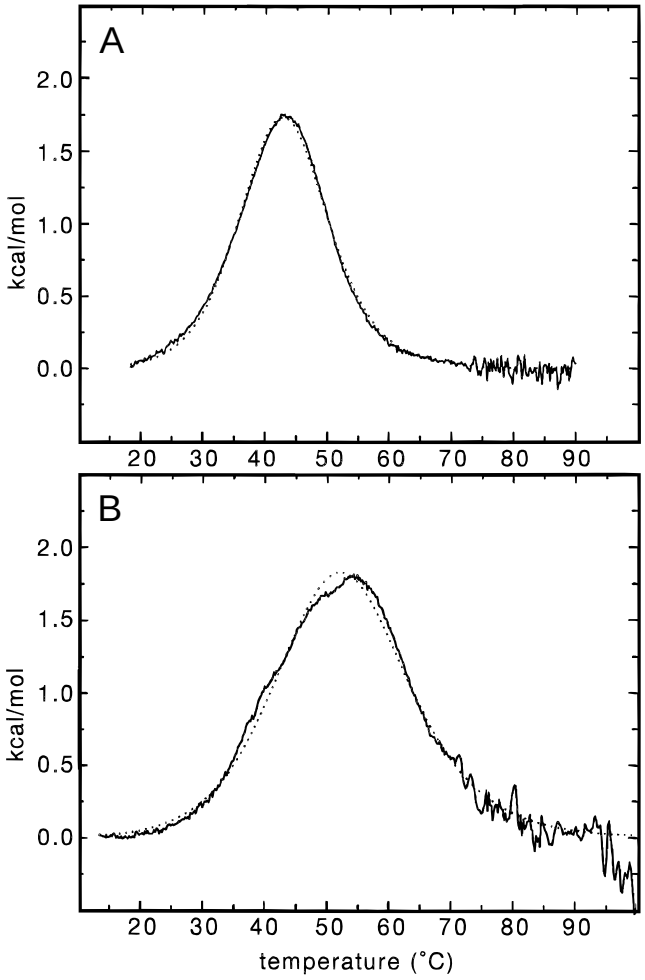

Fig. 1. Thermal stability of (**A**) E-domain and (**B**) E–D fragments of protein A. DSC was performed on protein solutions containing 50 mM sodium acetate, pH 5.0 at a heating rate of 1 °C/min. The solid lines are the observed melting curves corrected for the baseline heat capacity and normalized to the amount of protein in the calorimeter cell (0.9 mM E-domain, 0.6 mM E–D). Dashed lines represent nonlinear least-squares analysis of the transitions using a non-two-state model yielding thermodynamic parameters T_m = 43.0 °C, ΔH_{cal} = 33 kcal mol^{-1} and ΔH_{VH} = 42 kcal mol^{-1} for E-domain, and T_m = 51.5 °C, ΔH_{cal} = 48.5 and ΔH_{VH} = 29.3 kcal mol^{-1} for the E–D fragment.

Calorimetric measurement of protein A binding to antibody

Titration experiments with the two immunoglobulin binding domain fragment of protein A (E–D) are used to illustrate typical calorimetric data for binding to either hu4D5 Fab (Fig. 2A) or the intact antibody (Fig. 2B). In these experiments, the antibody solution was put in the calorimeter cell and titrated with a concentrated solution of protein A fragment. Binding to hu4D5 Fab can be described by a single class of binding sites model with n = 0.5 ± 0.1, K_a = 2.7 ± 0.5 $\times$ 10^5 M^{-1}, and ΔH = −14.1 ± 1.3 kcal mol^{-1}. A value of 0.5 for n suggests that both the E- and D-domains are functional for Fab binding simultaneously. Differences in Fab binding affinity between the two domains or evidence for cooperativity in binding are not detected by calorimetry suggesting that these are equivalent, noninteracting sites. As shown in Table 1, similar experiments with the isolated E-domain support

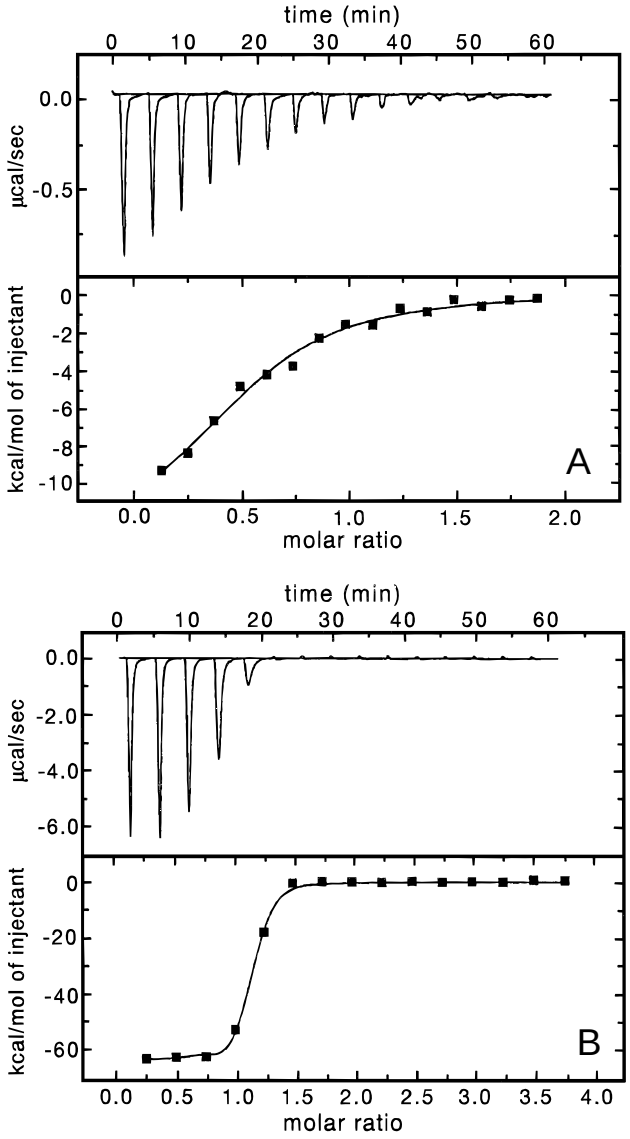

Fig. 2. Titration calorimetric measurement of E–D binding to hu4D5 (**A**) Fab and (**B**) antibody. See Materials and methods for details.

this conclusion. The ΔH for E-domain binding is half that measured for titration of Fab with E–D (-7.1 compared with -14.1 kcal mol^{-1}, respectively) as expected for equivalent, noninteracting sites. The affinity of E-domain for binding to the isolated V_H domain was within two-fold of that measured for Fab binding (Table 1) indicating that the E-domain binding site resides solely on V_H. The more exothermic ΔH of binding observed for the V_H domain relative to the Fab (-12.6 and -7.1 kcal mol^{-1}, respectively) may reflect the oligomerization state of V_H. At the concentrations used in the calorimetry experiments (34 μM), V_H is an equilibrium mixture of monomer and dimer (R.F. Kelley, unpubl. results). E-domain binding could perturb this equilibrium such that a portion of the ΔH measured for binding is contributed by V_H association.

Binding of hu4D5 Fab to intact protein A can also be described by a single class of binding sites having a K_a comparable to that measured for E–D or E-domain binding. Protein A appears to have 3–4 binding sites for Fab with the average ΔH somewhat larger than measured for E-domain binding. Binding experiments with full length protein A tended to give larger standard errors which we believe reflects the heterogeneity of the protein A preparation.

In contrast to results with E-domain, no binding to Fab was observed for Z-domain. Z-domain was competent for Fc binding as shown by titration experiments with ch4D5 MAb (Table 1). Since Fab fragments made from ch4D5 MAb cannot be purified on protein A-Sepharose (Kelley et al., 1992), this MAb (IgG1) does not appear to have a protein A binding site on V_H. Thus, the measured parameters for Z-domain interaction with ch4D5 MAb are presumed to reflect Fc binding. E-domain binding to Fc was determined by titrating an immunoadhesin (Capon et al., 1989) having the TNF receptor extracellular domain fused to the same human IgG1 Fc present in ch4D5 MAb. The ΔH values measured for Z- and E-domain binding to Fc are nearly identical, but a slightly larger binding constant was determined for E-domain compared with Z-domain binding to Fc. E-domain binding to TNFR-IgG gave a stoichiometry of 2.2 suggesting that both potential sites on the symmetrical Fc are functional in binding. Z-domain binding to ch4D5 MAb gave a smaller value for *n*, which most likely reflects errors in the concentration determination for ch4D5 MAb.

E-domain binding to the Fc fragment appears to be at least 50-fold higher affinity than the interaction of E-domain with the Fab fragment. The ΔG calculated from the binding constant for E-domain binding to Fab is -7.3 kcal mol^{-1}, which indicates that the entropy change for this process is about zero (ΔH is -7.1 kcal mol^{-1}). By comparison, a ΔG of -9.6 kcal mol^{-1} is calculated for E-domain binding to Fc by assuming a K_a of 1×10^7 M^{-1} (consistent with the value obtained by BIAcore measurements; Starovasnik et al., 1996). Since the ΔH of binding is -24.6 kcal mol^{-1}, this implies a large and unfavorable ΔS ($-T\Delta S$ = 15 kcal mol^{-1} at 25.5 °C; $\Delta S = -50$ cal K^{-1} mol^{-1}) upon binding. This thermodynamic comparison suggests that there are fundamental differences in the mechanism of E-domain binding to Fab and Fc sites.

Titration of hu4D5 MAb with the E–D fragment of protein A (Fig. 2B) gave a large, exothermic ΔH and an affinity that was too great to determine by calorimetry. Upon removal from the calorimeter cell, the MAb/E–D mixture was noticeably turbid. hu4D5 MAb has four potential protein A binding sites: one on each Fab arm and two on the Fc portion. Surprisingly, the calorimetric titration yielded a stoichiometry of 1.0. Given the apparent aggregation of the MAb/E–D complex, it seems likely that the E–D fragment can crosslink IgG molecules which may prevent full occupancy of all the binding sites.

Competition between Fab and Fc for E-domain binding

To determine whether Fab and Fc bind to overlapping sites on E-domain, two kinds of competition experiments were performed. In the first experiment, affinity chromatography on IgG-Sepharose was employed to assess competition. Addition of a 10-fold molar excess of Fab did not inhibit binding of E-domain to a column of IgG-Sepharose (data not shown). Indeed, after washing off unbound material, Fab coeluted with E-domain upon treatment of the column with 0.1 M glycine-HCL, pH 3. Control experiments showed that Fab did not bind to the IgG-Sepharose column in the absence of E-domain. No binding of Fab to the IgG-Sepharose column was observed in the presence of Z-domain, which does not bind hu4D5

Table 1. *Thermodynamic parameters for protein A binding to hu4D5 antibody*[a]

Protein	Titrant	n	$K_a \times 10^{-5}$ M^{-1}	ΔH (kcal mol^{-1})
Experiments with full length protein A[b]				
8 μM hu4D5 Fab[c]	119 μM protein A	0.26 ± 0.02	1.0 ± 0.1	−40.9 ± 4.3
8 μM protein A	571 μM hu4D5 Fab	2.9 ± 0.1	5.5 ± 0.5	−10.7 ± 0.2
4 μM protein A	571 μM hu4D5 Fab	3.5 ± 0.5	1.5 ± 0.5	−13.8 ± 2.4
Experiments with E–D two domain fragment				
20 μM hu4D5 Fab	563 μM E–D	0.5 ± 0.1	2.7 ± 0.5	−14.1 ± 1.3
10 μM hu4D5 MAb[d]	563 μM E–D	1.02 ± 0.01	>100	−63.6 ± 0.5
10 μM ch4D5 MAb[e]	563 μM E–D	0.65 ± 0.01	>100	−49.4 ± 0.4
Experiments with individual domains of protein A				
10 μM ch4D5 MAb	230 μM Z-domain	1.4 ± 0.1	36 ± 7	−24.3 ± 0.1
4.0 μM TNFR-IgG[f]	1.15 mM E-domain	2.2 ± 0.1	>100	−24.6 ± 0.6
20 μM E-domain	330 μM hu4D5 Fab	1.0 ± 0.1	2.0 ± 0.3	−7.1 ± 0.4
34 μM V_H domain	863 μM E-domain	1.2 ± 0.1	1.0 ± 0.1	−12.6 ± 0.6
Experiment to test for competition between Fc and Fab for E-domain binding				
20 μM E-domain with 20 μM TNFR-IgG	330 μM hu4D5 Fab	1.0 ± 0.1	2.1 ± 0.3	−6.6 ± 0.3

[a]Titrations performed as described in Materials and methods. The ΔH values were calculated on the basis of the molar concentration of the protein in the calorimeter cell.
[b]Full-length protein A contains five homologous domains.
[c]hu4D5 Fab contains one V_H3 protein A binding domain.
[d]hu4D5 MAb contains potentially two V_H3 and two IgG1 Fc protein A binding sites.
[e]ch4D5 MAb contains two IgG1 Fc protein A binding sites and no Fab binding site.
[f]TNFR-IgG contains two IgG1 Fc protein A binding sites.

Fab. These results suggest that E-domain can bind simultaneously to Fab and Fc sites.

In the second experiment, the binding of Fab to E-domain in the presence of an excess of TNFR-IgG was determined by calorimetry. This experiment employed a twofold excess of Fc binding sites over E-domain. As shown in Table 1, nearly identical binding parameters are obtained for Fab binding to E-domain whether in the presence or absence of TNFR-IgG. Since the affinity of E-domain for Fc is greater than for Fab, a much reduced binding constant should have been observed in this experiment if the binding sites for Fab and Fc were overlapping. Instead this result indicates that the binding sites involve distinct sets of residues that are sufficiently separated to allow binding of both Fab and Fc.

NMR chemical shift mapping of the Fv binding site on E-domain

Comparison of resonance frequencies in free and bound states has been used previously to identify protein–protein interaction sites (Chen et al., 1993; van Nuland et al., 1993). The chemical shift of a nucleus is highly sensitive to its local electronic environment, thus when residues on the surface of a protein come in contact with a binding partner they typically experience a change in chemical shift. Chemical shift changes result directly from contact with the binding partner or indirectly from conformational changes associated with the binding event (Foster et al., 1998). In general, the area described by chemical shift mapping is larger than the region directly in contact due to the fact that residues on the periphery of a binding site experience a change in local environment induced by neighboring contact residues (Spitzfaden et al., 1992). This technique has been used previously to identify the areas on *Streptococcal* protein G that interact with Fc (Gronenborn & Clore, 1993) and Fab (Lian et al., 1994) fragments and to define the region on a V_H3 domain that interacts with protein A domains A–B (Riechmann & Davies, 1995).

^{15}N-labeled E-domain was titrated with unlabeled Fv fragment from hu4D5 to identify which residues of E-domain have chemical shifts that are perturbed upon binding. The Fv fragment was chosen for this experiment because the E-domain/Fab complex would be less amenable to NMR structural analysis. Although the binding site is contained solely within the V_H chain (Table 1), the V_H/V_L heterodimer (Fv fragment) was used in these experiments due to the poor solubility and aggregation of V_H alone. Figure 3 shows a segment of the E-domain HSQC spectrum with differing amounts of unlabeled Fv present. When there is a less than stoichiometric amount of Fv present, two sets of E-domain peaks are observed representing free and bound forms of E-domain in slow exchange. The new (bound) peaks are significantly broader than the initial peaks. No "free" peaks are observed after a 1:1 ratio of E-domain:Fv is obtained, although the linewidths of the "bound" peaks continue to narrow with the addition of excess Fv. Slow exchange behavior is observed even for nuclei where the frequencies of the free and bound peaks differ by less than 5 Hz, indicating that the lifetime of the bound state is >200 ms.

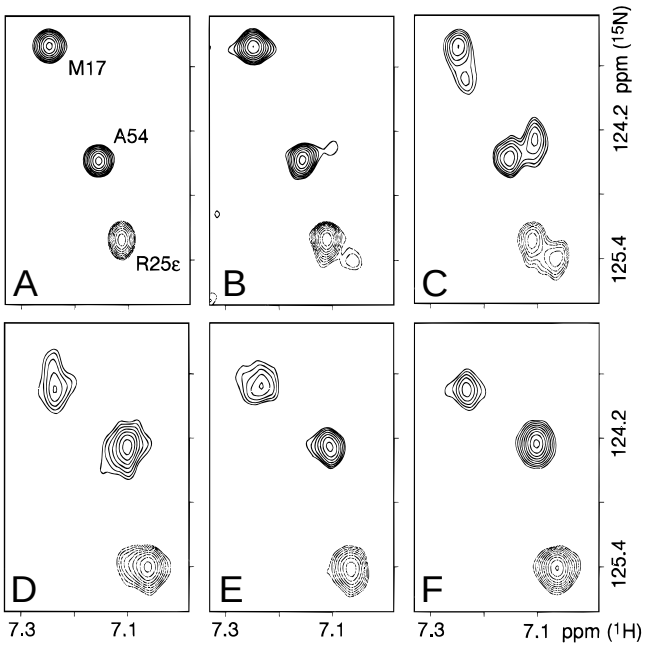

Fig. 3. Titration of unlabeled Fv into ^{15}N-labeled E-domain. A small region of the two-dimensional ^{1}H/^{15}N-HSQC spectrum of ^{15}N-labeled E-domain in the presence of a (**A**) 1:0, (**B**) 1:0.25, (**C**) 1:0.50, (**D**) 1:0.75, (**E**) 1:1.0, and (**F**) 1:1.25 molar ratio of E-domain to Fv fragment. Amide peaks from residues Met17 and Ala54 and the ϵ amino group of Arg25 (folded in these spectra) are shown. Note that separate free and bound peaks are observed.

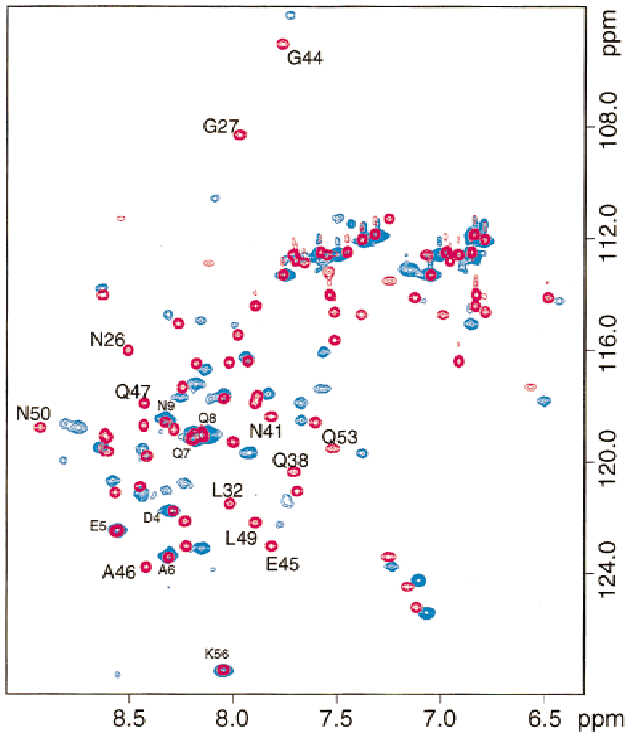

Fig. 4. ^{1}H/^{15}N-HSQC spectrum of ^{15}N-labeled E-domain in the absence (red) and presence (blue) of unlabeled Fv. Spectra were acquired as indicated in Materials and methods. Peaks undergoing a large change in chemical shift are labeled (see text for details). Peaks from the N- and C-terminal ends of E-domain that are not perturbed upon binding are also labeled, but using a smaller font.

An overlay of the ^{1}H/^{15}N-HSQC spectrum of E-domain in the free and Fv-bound states is shown in Figure 4. Eighty percent of the E-domain backbone amide peaks undergo at least a slight change in chemical shift upon addition of Fv. Peaks have been arbitrarily classified as undergoing a large change in chemical shift if there is no peak observed in the spectrum of the complex within 0.1 ppm (^{1}H) and 0.5 ppm (^{15}N) of the peak in the unbound state; these residues are colored red on the ribbon diagram of E-domain in Figure 5 and map to the helix-2/helix-3 face. In addition, side-chain NH_2 groups of asparagine and glutamine residues that undergo large changes in chemical shift upon Fv-binding also map to helices 2 and 3 exclusively (Fig. 5). Residues at the N- and C-terminal ends (i.e., residues 4–9 and 56; residues 1–3 are not observed under these conditions) of E-domain show no change in chemical shift upon binding and maintain relatively sharp linewidths in the Fv-bound state indicating that the local environments of these residues are unchanged by Fv-binding. The fact that the remaining E-domain peaks experience at least a slight chemical shift perturbation upon Fv-binding could be due to the limited stability of E-domain. The chemical shifts observed for the free form of E-domain are a population weighted average of the chemical shifts in the folded and unfolded states; Fv-binding would perturb this equilibrium by selecting for the folded state. Alternatively, there could be a small rearrangement of the three-helix bundle structure in the bound state.

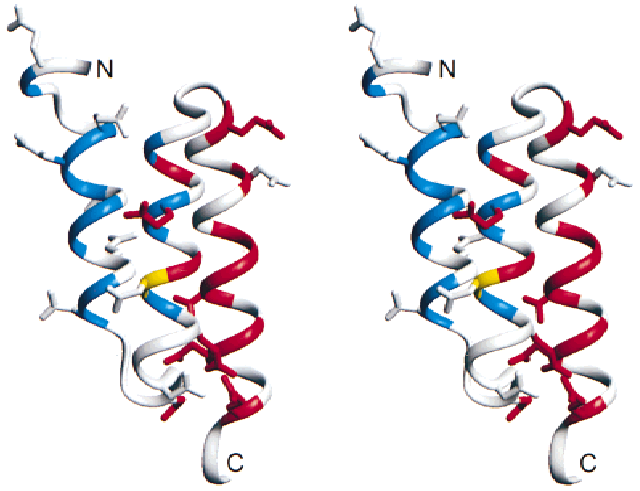

Fig. 5. Chemical shift map of the Fv binding surface on E-domain. Residues with backbone amide ^{1}H and/or ^{15}N resonances that undergo a large change in chemical shift upon Fv-binding are colored red on a ribbon diagram of the E-domain structure. For comparison, residues that contain atoms in contact with Fc in the crystal structure of the B-domain/Fc complex (Deisenhofer, 1981) are colored blue. The one residue, Asn26, that both undergoes a large change in chemical shift upon Fv binding and makes contact with Fc in the B-domain/Fc crystal structure is colored yellow. Side chains for all asparagine and glutamine residues are shown; those colored red have side-chain NH_2 groups that undergo a large change in chemical shift upon Fv-binding. This figure was generated using the program INSIGHT II (Molecular Simulations, Inc.).

Discussion

We have examined the stability and variable region binding properties of full length protein A, a two-domain E–D fragment and the

isolated E-domain of protein A. Thermal denaturation by DSC indicates E-domain is relatively unstable, melting with a T_m of 43 °C. In contrast, Z-domain is much more stable with a T_m of ~70 °C (Starovasnik et al., 1997). This difference is surprising given the high sequence and overall structural similarity between the E- and Z-domains (there are only 11 amino acid differences out of 50 residues, not counting the disordered N-terminal residues; Starovasnik et al., 1996; Tashiro et al., 1997). The low stability of E-domain may be, in part, due to the fact that there are two glycine residues (Gly27 and Gly44) within α-helices 2 and 3 that are alanine residues in the corresponding positions in Z-domain. Mutagenesis studies are underway to identify the residues responsible for the stability difference.

Both E- and D-domains were found to be capable of binding V_H3-containing Fab, consistent with previous reports (Roben et al., 1995; Jansson et al., 1998). Comparison of the isolated E-domain and the E–D fragment suggests that the two domains bind as independent, noninteracting sites with association constants of $\sim 2 \times 10^5$ M^{-1}. Jansson et al. (1998) report a 10-fold higher affinity based on surface plasmon resonance measurements of the binding of an anti-p53 scFv to immobilized protein A fragments. In addition to the variation resulting from the different methods used, the affinity does vary with the specific V_H3-containing Fab or Fv measured (R.F. Kelley, unpubl. results). We chose to work with fragments of the humanized anti-HER2 antibody, hu4D5, because it expresses extremely well and the crystal structures for its Fab and Fv fragments have been solved (Eigenbrot et al., 1993).

The calorimetric measurements indicate that E-domain binding to Fab occurs with a negligible entropy change, whereas there is a large, unfavorable ΔS for E-domain binding to Fc. In neither case is there a large and favorable ΔS as might be expected for a dominant contribution to binding from the hydrophobic effect (Tanford, 1980). A variety of factors (Sturtevant, 1977) could account for the difference in ΔS between Fc and Fab binding. The mass of the 2:1 E-domain:Fc complex is larger than the 1:1 E-domain:Fab complex; a larger change in mass upon binding should increase the entropic penalty from the loss of translational and rotational degrees of freedom. A decrease in the rotational freedom of side chains, a tightening of vibrational modes, and/or changes in backbone dynamics can contribute to an unfavorable ΔS. In addition, if binding reduces the number of isoenergetic conformations of the protein then a negative ΔS would result. The free E-domain structure is not significantly different than the Fc-bound B-domain structure except for the orientation of the side chain of Phe11 (Starovasnik et al., 1996). Given that this side chain undergoes rapid exchange between $\chi 1$ rotamers in the unbound state, it is unlikely that this side chain alone could account for much of the large entropy cost upon binding. Similarly, there is very little difference between the free Fc and B-domain/Fc complex structures except for the side-chain conformation of Ile253 (Deisenhofer, 1981).

Comparison of Fc and Fv binding sites on E-domain

NMR chemical shift mapping of the Fv-binding region on E-domain implicates the helix-2/helix-3 face as the site of interaction. The Fc-binding site on E-domain is expected to be essentially identical to that observed in the crystal structure of the B-domain/Fc complex given the high sequence and structural similarity in this region (Starovasnik et al., 1996). The Fc- and Fv-binding regions are clearly distinct from one another (Fig. 5); only one residue, Asn26, is found to have both an amide peak that undergoes a large change in chemical shift upon Fv binding and have atoms in contact with Fc in the B-domain/Fc complex structure (Deisenhofer, 1981). Given that chemical shift mapping typically describes a region slightly larger than the contact site and that Asn26 is on the periphery of each of the binding regions, this result is consistent with the fact that Fc and Fab do not compete with one another for binding.

Jansson et al. (1998) comment on the importance of Gly27 in a report that investigated Fab binding properties of all five native protein A domains and Z-domain. Z-domain only differs from B-domain at one position within the structured region of the construct: the glycine corresponding to Gly27 (that is conserved in all native protein A domains) is replaced by alanine. They report that all five native domains show roughly comparable binding affinity for the Fab studied, but Z-domain binding was barely detectable. The loss in binding due to the alanine could be due to a steric clash with the Fab interface introduced by the methyl group or because a conformational change requiring glycine in helix-2 is necessary for high affinity binding. Z-domain and E-domain have very similar structures in this region (Starovasnik et al., 1996; Tashiro et al., 1997), thus there appears to be nothing special about having glycine in this position in the unbound state. The methyl group of the alanine in Z-domain lies within the Fv-binding region defined here and further implicates the helix-2/helix-3 face as the site of Fv binding.

The surface characteristics of the helix-1/helix-2 face and helix-2/helix-3 face of E-domain are depicted in Figure 6. The helix-1/helix-2 face involved in Fc-binding is largely hydrophobic, bordered by two positive charges (Fig. 6A). In striking contrast, the helix-2/helix-3 face involved in Fv-binding is highly negatively charged with a small hydrophobic region in the center (Fig. 6B).

The region of the V_H domain that interacts with protein A has also been identified. Clearly the binding site is not within the V_H/V_L interface or the conventional antigen binding site since the presence or absence of V_L or antigen does not usually affect binding (Table 1; Young et al., 1984). Riechmann and Davies have mapped residues involved in protein A binding by NMR chemical shift perturbation (using a two-domain A–B fragment) and have identified a binding surface contained within framework regions 1 and 3 (Riechmann & Davies, 1995). This surface of V_H3 from the structure of hu4D5 Fv is illustrated in Figure 6C and depicts a positively charged surface complementary to the negative charge present on the Fv-binding surface of E-domain defined here.

In summary, we have shown that an individual 56 amino acid protein A domain contains two nonoverlapping protein binding sites. The Fv binding site lies within the helix-2/helix-3 face of E-domain, whereas the Fc binding site is localized to the helix-1/helix-2 face. The two binding sites on E-domain display very different surface characteristics which might contribute to the different thermodynamic parameters determined for Fc and Fv binding. Complete structure determination of the E-domain/Fv complex is ongoing to define the specific orientation of the domains in the bound state and to further define essential elements of this protein–protein interaction.

Materials and methods

Materials

S. aureus protein A was purchased from Calbiochem (La Jolla, California); the protein was used without further purification, al-

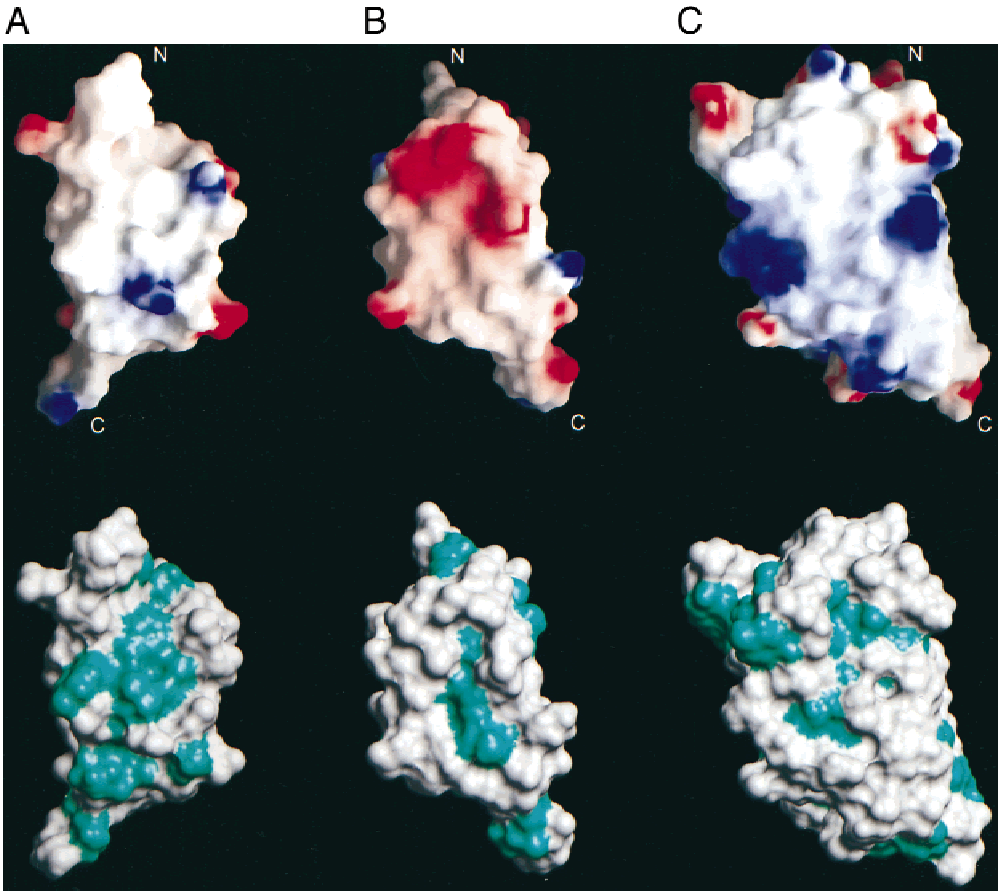

Fig. 6. The solvent accessible molecular surface color coded according to electrostatic surface potential (top row: red, −9 kT; white, 0 kT; blue, +9 kT) and hydrophobic surface (bottom row: ala, cys, ile, leu, met, phe, pro, tyr, trp, val residues colored green) of the (**A**) Fc binding face of E-domain, (**B**) Fv binding face of E-domain, and (**C**) V_H surface implicated in protein A binding by previous chemical shift mapping studies (Riechmann & Davies, 1995). The view shown in **B** differs from that in **A** by a 140° rotation about the vertical axis. The V_L domain is not shown in (**C**), but would be behind the V_H domain with the CDR loops located at the top in this view. All views were chosen to emphasize residues in contact (**A**) or that undergo chemical shift perturbations (**B,C**) in the relevant complex. E-domain and Fv coordinates used to generate this figure and the previous figure are from Protein Data Bank files 1EDK (Starovasnik et al., 1996) and 1FVC (Eigenbrot et al., 1993), respectively. The top row of this figure was generated using the program GRASP (Nicholls, 1992); the bottom row was generated using the program INSIGHT II (Molecular Simulations, Inc.).

though the protein A appeared heterogeneous by SDS-PAGE (not shown). ch4D5 and hu4D5 Mab are the chimeric and fully humanized versions of a monoclonal antibody directed against the extracellular domain of human epidermal growth factor receptor-2 (HER-2) (Carter et al., 1992) and were provided by G. Blank (Genentech, Inc., South San Francisco, California). The Fab fragment and isolated V_H domain of 4D5 were obtained by recombinant expression and purification as described previously (Kelley et al., 1992). TNFR-IgG is an immunoadhesin (Capon et al., 1989) consisting of the tumor necrosis factor receptor extracellular domain fused to an IgG1 Fc and was provided by S. Chamow (Genentech, Inc.).

Production of protein A and antibody fragments

The plasmids pRIT32, encoding the entire protein A gene, and pZAP2, a plasmid designed for *E. coli* expression of a Z-domain–alkaline phosphatase fusion protein, were constructed by Dr. Lars Abrahmsen (Pharmacia & Upjohn, Sweden). pZAP2 uses the alkaline phosphatase (phoA) promoter and stII signal sequence to cause secretion of the fusion protein and also has an f1 origin for production of single-stranded DNA. Cassette mutagenesis (Wells et al., 1985) was used to place a stop codon at the end of Z-domain and to delete the alkaline phosphatase part of the fusion protein, thus generating the plasmid pZCT. This Z-domain construct is similar to that initially described by Nilsson et al. (1987) and differs from the native B-domain by having an additional six amino acids at the N-terminus, what would be the N-terminal alanine (now residue 7) replaced by valine and Gly29 (or 35 if numbered from the N-terminus of this construct) replaced by alanine to remove a potential deamidation site (see Fig. 1 of Nilsson et al., 1987 for sequence comparison). The Z-domain portion of pZCT was replaced with a fragment encoding the E–D domains by first performing a PCR reaction on pRIT32, then cleaving the PCR product with MluI and SphI restriction enzymes (New England Biolabs, Beverly, Massachusetts), followed by ligation of the fragment with MluI/SphI digested pZCT. This yielded the plasmid pSED, which enables secretion of the E–D fragment from *Escherichia coli* using

the phoA promoter. A similar plasmid for secretion of E-domain alone (pSE) was obtained by using oligonucleotide-directed mutagenesis (Kunkel et al., 1987) to insert a stop codon at the end of E-domain. pA19.2, a plasmid designed for phoA-stII directed secretion from *E. coli* of the Fv fragment of hu4D5, was constructed by P. Carter (Genentech, Inc.).

The sequences of pZCT, pSED, pSE, and pA19.2 were confirmed by dideoxynucleotide sequencing of the single stranded form of the plasmid. Protein A fragments E–D, Z-domain, E-domain, and ^{15}N-labeled E-domain were expressed by secretion from *E. coli* and purified by chromatography on IgG-Sepharose as described previously (Starovasnik et al., 1996). All four proteins had N-termini and molecular weights consistent with their sequences, as determined by automated Edman degradation and electrospray ionization mass spectrometry, respectively. As expected based on the structures determined previously for the E-, B-, and Z-domains of protein A (Deisenhofer, 1981; Gouda et al., 1992; Tashiro & Montelione, 1995; Starovasnik et al., 1996; Tashiro et al., 1997), these immunoglobulin-binding fragments displayed far UV-circular dichroism (CD) spectra characteristic of helical proteins (data not shown). hu4D5 Fv was expressed by secretion from *E. coli* and purified essentially as described for the Fab fragments of 4D5 (Kelley et al., 1992).

Differential scanning calorimetry

Thermal denaturation experiments were performed on a Microcal, Inc. (Northampton, Massachusetts) MC-2 differential scanning calorimeter. Protein samples were prepared for measurement by dialysis vs. a solution containing 50 mM sodium acetate, pH 5.0. A heating rate of 1 °C/min was employed. Melting profiles were baseline corrected, normalized to protein concentration, and analyzed by nonlinear regression using software supplied by the manufacturer. The calorimetric enthalpy (ΔH_{cal}) was determined from the area of the heat absorption peak, whereas the effective or van't Hoff enthalpy (ΔH_{VH}), which describes the temperature dependence of the equilibrium constant for denaturation, was evaluated from the fractional amount of heat absorbed as a function of temperature (Privalov, 1979). For two-state denaturation, $\Delta H_{cal}/\Delta H_{VH} = 1$.

Isothermal titration calorimetry

Microcalorimetric measurements of the interaction of protein A domains with antibody fragments were performed on a Microcal, Inc. OMEGA titration calorimeter operated as described previously (Kelley & O'Connell, 1993). Protein solutions were prepared by exhaustive dialysis vs. a buffer solution of 20 mM sodium phosphate, pH 7.5, 100 mM NaCl. Protein solution, at a concentration of 4–40 μM, was loaded into the 1.4 mL calorimeter cell and titrated by 12–15 equal volume injections of a concentrated solution of binding partner ("titrant"). A 100 μL injection syringe was used, and the stirring rate was 400 RPM. All measurements were performed after thermal equilibrium at 25.5 °C had been obtained. The heat effect for each injection was calculated by computer integration of the observed heat flux. Heats of titrant dilution were determined in separate experiments and subtracted from the integrated heats to obtain the heat of binding. These binding isotherms were analyzed by nonlinear regression analysis, using software supplied by the manufacturer, to calculate the independent parameters n, K_a, and ΔH.

NMR spectroscopy

NMR spectra were acquired on a Bruker AMX-500 spectrometer at 25 °C. ^{1}H/^{15}N-heteronuclear single-quantum coherence (HSQC) spectra were acquired using spin-lock purge pulses for water suppression (Messerle et al., 1989). Quadrature detection in t_1 was obtained using time proportional phase incrementation (Marion & Wüthrich, 1983). Chemical shifts were referenced to internal DSS.

Chemical shift mapping of the Fv binding site on E-domain

Unlabeled Fv in the presence of phosphate buffered saline (PBS), pH 5.8, 0.1 mM NaN_3, 0.1 mM EDTA, 92% H_2O, 8% D_2O was titrated into ^{15}N-labeled E-domain in the same buffer and monitored by 2D ^{1}H/^{15}N-HSQC spectra at 25 °C. The initial E-domain concentration was 1.6 mM; five additions of 0.25 molar equivalents were made from a 0.93 mM stock of Fv such that the final sample contained 0.4 mM ^{15}N-labeled E-domain, 0.5 mM unlabeled Fv. Spectra shown in Figure 4 were acquired with 8 and 512 scans/increment for free and Fv-bound E-domain, respectively, and were collected with a 1,250 Hz ^{15}N spectral width acquired over 200 t_1 increments.

Acknowledgments

We thank Dr. Lars Abrahmsen for the gift of the plasmids encoding protein A (pRIT32) and Z-domain (pZAP2), Dr. Paul Carter for the gift of the plasmid encoding hu4D5 Fv (pA19.2), and Dr. Nicholas Skelton for many helpful discussions.

References

Braisted AC, Wells JA. 1996. Minimizing a binding domain from protein A. *Proc Natl Acad Sci USA 93*:5688–5692.

Capon DJ, Chamow SM, Mordenti J, Marsters SA, Gregory T, Mitsuya H, Byrn RA, Lucas C, Wurm FM, Groopman JE, Broder S, Smith DH. 1989. Designing CD4 immunoadhesins for AIDS therapy. *Nature 337*:525–531.

Carter P, Presta L, Gorman CM, Ridgway JBB, Henner D, Wong WLT, Rowland AM, Kotts C, Carver ME, Shepard HM. 1992. Humanization of an anti-p185HER2 antibody for human cancer therapy. *Proc Natl Acad Sci USA 89*:4285–4289.

Cedergren L, Andersson R, Jansson B, Uhlen M, Nilsson B. 1993. Mutational analysis of the interaction between staphylococcal protein A and human IgG1. *Protein Eng 6*:441–448.

Chen Y, Reizer J, Saier MHJ, Fairbrother WJ, Wright PE. 1993. Mapping of the binding interfaces of the proteins of the bacterial phosphotransferase system, HPr and IIA^{glc}. *Biochemistry 32*:32–37.

Deisenhofer J. 1981. Crystallographic refinement and atomic models of human Fc fragment and its complex with fragment B of protein A from *Staphylococcus aureus* at 2.9- and 2.8-Å resolution. *Biochemistry 20*:2361–2370.

Eigenbrot C, Randal M, Presta L, Carter P, Kossiakoff AA. 1993. X-ray structures of the antigen-binding domains from three variants of humanized anti-p185^{HER2} antibody 4D5 and comparison with molecular modeling. *J Mol Biol 229*:969–995.

Foster MP, Wuttke DS, Clemens KR, Jahnke W, Radhakrishnan I, Tennant L, Reymond M, Chung J, Wright PE. 1998. Chemical shift as a probe of molecular interfaces: NMR studies of DNA binding by the three amino-terminal zinc finger domains from transcription factor IIIA. *J Biomol NMR 12*:51–71.

Gouda H, Torigoe H, Saito A, Sato M, Arata Y, Shimada I. 1992. Three-dimensional solution structure of the B domain of staphylococcal protein A: Comparisons of the solution and crystal structures. *Biochemistry 31*:9665–9672.

Gronenborn AM, Clore GM. 1993. Identification of the contact surface of a streptococcal protein G domain complexed with a human Fc fragment. *J Mol Biol 233*:331–335.

Hjelm H, Sjödahl J, Sjöquist J. 1975. Immunologically active and structurally similar fragments of protein A from Staphylococcus aureus. *Eur J Biochem 57*:395–403.

Jansson B, Uhlén M, Nygren P-A. 1998. All individual domains of staphylococcal protein A show Fab binding. *FEMS Immunol Med Microbiol 20*: 69–78.

Jendeberg L, Persson B, Andersson R, Karlsson R, Uhlén M, Nilsson B. 1995. Kinetic analysis of the interaction between protein A domain variants and human Fc using plasmon resonance detection. *J Mol Recognit 8*:270–278.

Kelley RF, O'Connell MP. 1993. Thermodynamic analysis of an antibody functional epitope. *Biochemistry 32*:6828–6835.

Kelley RF, O'Connell MP, Carter P, Presta L, Eigenbrot C, Covarrubias M, Snedecor B, Bourell JH, Vetterlein D. 1992. Antigen binding thermodynamics and anti-proliferative effects of chimeric and humanized anti-p185^{HER2} antibody fragments. *Biochemistry 31*:5434–5441.

Kunkel TA, Roberts JD, Zakour RA. 1987. Rapid and efficient site-specific mutagenesis without phenotypic selection. *Methods Enzymol 154*:367–382.

Langone JJ. 1982. Protein A of *Staphylococcus aureus* and related immunoglobulin receptors produced by streptococci and Pneumonococci. *Adv Immunol 32*:157–252.

Lian L-Y, Barsukov IL, Derrick JP, Roberts GCK. 1994. Mapping the interactions between streptococcal protein G and the Fab fragment of IgG in solution. *Nat Struct Biol 1*:355–357.

Löfdahl S, Guss B, Uhlén M, Philipson L, Lindberg M. 1983. Gene for staphylococcal protein A. *Proc Natl Acad Sci USA 80*:697–701.

Marion D, Wüthrich K. 1983. Application of phase sensitive two-dimensional correlated spectroscopy (COSY) for measuring ^{1}H-^{1}H spin-spin coupling constants in proteins. *Biochem Biophys Res Commun 113*:967–974.

Messerle BA, Wider G, Otting G, Weber C, Wüthrich K. 1989. Solvent suppression using a spin-lock in two- and three-dimensional NMR spectroscopy in H_2O solution. *J Magn Reson 85*:608–613.

Moks T, Abrahmsen L, Nilsson B, Hellman U, Sjöquist J, Uhlén M. 1986. Staphylococcal protein A consists of five IgG-binding domains. *Eur J Biochem 156*:637–643.

Nicholls A. 1992. *GRASP: Graphical representation and analysis of surface properties*. New York: Columbia University.

Nilsson B, Moks T, Jansson B, Abrahmsén L, Elmblad A, Holmgren E, Henrichson C, Jones TA, Uhlén M. 1987. A synthetic IgG-binding domain based on staphylococcal protein A. *Protein Eng 1*:107–113.

Potter KN, Li Y, Capra JD. 1996. Staphylococcal protein A simultaneously interacts with framework region 1, complementarity-determining region 2, and framework region 3 on human VH3-encoded Igs. *J Immunol 157*:2982–2988.

Privalov PL. 1979. Stability of proteins: Small globular proteins. *Adv Protein Chem 33*:167–241.

Randen I, Potter KN, Li Y, Thompson KM, Pascual V, Førre Ø, Natvig JB, Capra JD. 1993. Complementarity-determining region 2 is implicated in the binding of staphylococcal protein A to human immunoglobulin VHIII variable regions. *Eur J Immunol 23*:2682–2686.

Riechmann L, Davies J. 1995. Backbone assignment, secondary structure and protein A binding of an isolated, human antibody VH domain. *J Biomol NMR 6*:141–152.

Roben PW, Salem AN, Silverman GJ. 1995. VH3 family antibodies bind domain D of staphylococcal protein A. *J Immunol 154*:6437–6445.

Romagnani S, Giudizi MG, Del Prete G, Maggi E, Biagiotti R, Almerigogna F, Ricci M. 1982. Demonstration on protein A of two distinct immunoglobulin-binding sites and their role in the mitogenic activity of *Staphylococcus aureus* Cowan I on human B cells. *J Immunol 129*:596–602.

Silverman GJ. 1998. B cell superantigens: Possible roles in immunodeficiency and autoimmunity. *Semin Immunol 10*:43–55.

Sjödahl J. 1976. Repetitive sequences in protein A from *Staphylococcus aureus*: Three highly homologous Fc-binding regions. *FEBS Lett 67*:62–67.

Sjödahl J. 1977a. Repetitive sequences in protein A from *Staphylococcus aureus*. Arrangement of five regions within the protein, four being highly homologous and Fc-binding. *Eur J Biochem 73*:343–351.

Sjödahl J. 1977b. Structural studies on the four repetitive Fc-binding regions in protein A from *Staphylococcus aureus*. *Eur J Biochem 78*:471–490.

Spitzfaden C, Weber HP, Braun W, Kallen J, Wider G, Widmer H, Walkinshaw MD, Wüthrich K. 1992. Cyclosporin A-cyclophilin complex formation. A model based on X-ray and NMR data. *FEBS Lett 300*:291–300.

Starovasnik MA, Braisted AC, Wells JA. 1997. Structural mimicry of a native protein by a minimized binding domain. *Proc Natl Acad Sci USA 94*:10080–10085.

Starovasnik MA, Skelton NJ, O'Connell MP, Kelley RF, Reilly D, Fairbrother WJ. 1996. Solution structure of the E-domain of Staphylococcal protein A. *Biochemistry 35*:15558–15569.

Sturtevant JM. 1977. Heat capacity and entropy changes in processes involving proteins. *Proc Natl Acad Sci USA 74*:2236–2240.

Tanford C. 1980. *The hydrophobic effect*. New York: Wiley-Interscience.

Tashiro M, Montelione GT. 1995. Structures of bacterial immunoglobulin-binding domains and their complexes with immunoglobulins. *Curr Opin Struct Biol 5*:471–481.

Tashiro M, Tejero R, Zimmerman DE, Celda B, Nilsson B, Montelione GT. 1997. High-resolution solution NMR structure of the Z domain of staphylococcal protein A. *J Mol Biol 272*:573–590.

Uhlén M, Guss B, Nilsson B, Gatenbeck S, Philipson L, Lindberg M. 1984. Complete sequence of the staphylococcal gene encoding protein A. A gene evolved through multiple duplications. *J Biol Chem 259*:1695–1702.

van Nuland NAJ, Kroon GJA, Dijkstra K, Wolters GK, Scheek RM, Robillard GT. 1993. The NMR determination of the IIA^{mtl} binding site on HPr of the *Escherichia coli* phosphoenol pyruvate-dependent phosphotransferase system. *FEBS Lett 315*:11–15.

Wells JA, Vasser M, Powers DB. 1985. Cassette mutagenesis: An efficient method for generation of multiple mutations at defined sites. *Gene 34*:315–323.

Young WW, Tamura Y, Wolock DM, Fox JW. 1984. Staphylococcal A binding to the Fab of mouse monoclonal antibodies. *J Immunol 133*:3163–3166.